

Influences of the Heme-Lysine Crosslink in Cytochrome P460 Over Redox Catalysis and Nitric Oxide Sensitivity

SUPPORTING INFORMATION

*Avery C. Vilbert, Jonathan D. Caranto, and Kyle M. Lancaster**

Department of Chemistry and Chemical Biology, Baker Laboratory, Cornell University, Ithaca, NY 14853

17th August 2018

Note added after first publication: This supplementary information file replaces that originally published on 7th November 2017 in which the experimental methods and references were missing.

TABLE OF CONTENTS

Experimental Methods	S2
Supplementary Figures	S6
Supplementary Tables	S14
References	S17

Experimental Methods

General considerations. Milli-Q water (18.2 M Ω ; Millipore) was used in all preparations of buffers and solutions. 1-(Hydroxyl-NNO-azoxy)-L-proline, disodium salt (Proli-NONOate) and disodium diazen-1-ium-1,2,2 triolate (Na₂N₂O₃, Angeli's salt) were purchased from Cayman Chemicals. Stock solutions of Proli-NONOate and Na₂N₂O₃ were prepared as described previously.¹ NH₂OH•HCl was purchased from Sigma-Aldrich. All other chemicals were purchased from VWR International and used as obtained. All reactions were prepared inside an MBraun Labstar glovebox under a N₂ atmosphere. All buffers were degassed with 3 cycles of vacuum for 20 min followed by sparging with N₂ for 20 min. Aliquots of protein were equilibrated in the glovebox for 2 h before the experiments. UV-vis absorption spectra were obtained using either a scanning Cary 60 UV-vis spectrometer or an Ocean Optics 2000+ high-resolution diode array spectrometer coupled to a KinTek SF-2004 stopped-flow apparatus. UV-vis scans using the Cary 60 UV-vis spectrometer spanned 200–800 nm with scan rates of 80 nm/s. Temperatures were controlled using a Peltier accessory. The Ocean Optics spectrometer spanned a usable range of 200–500 nm. The optical flow cell was 0.5 cm with a 3 ms mixing dead time. Before the experiments, the stopped-flow syringes were flushed with sodium dithionite (Na₂S₂O₄) for deoxygenation. The lines were then washed with deoxygenated buffer to rinse out the remaining Na₂S₂O₄. Temperatures were controlled by using a water jacket hooked to a recirculating water bath. Kinetics data were fit using v6.37 of the IgorPro software package (Wavemetrics).

Protein expression and purification. WT *N. europaea* cyt P460 was purified and expressed as previously described.¹ An expression system for Lys70Tyr cyt P460 was constructed via site-directed mutagenesis of the pET-22b+ vector bearing the gene for WT cyt P460. The Lys70Tyr expression plasmid was co-transformed with a pEC86 plasmid bearing the cyt c maturation genes ccmABCDFGH² (provided by H. B. Gray) into *Escherichia coli* strain BL21(DE3). A single colony was then used to inoculate a 3 mL starter culture of lysogeny broth supplemented with 100 μ g mL⁻¹ ampicillin and chloramphenicol. The starter culture was shaken at 200 rpm at 37 °C for 6 h. Then, 1.5 mL of starter culture was used to inoculate two 4 L Erlenmeyer flasks containing 1.5 L of Terrific Broth medium. The cells were grown with shaking at 200 rpm at 30 °C to an optical density at 600 nm of 0.7 \pm 0.1. The temperature was then decreased to 20 °C, and protein expression was induced by adding isopropyl β -D-1-thiogalactopyranoside to a final concentration of 0.4 mM. The cells were harvested via centrifugation as a pink pellet after 24 h, resuspended in 20 mM Tris containing 150 mM NaCl and 0.01% Triton X (pH 8.0), and lysed via sonication. The pink soluble lysate fraction was separated from cellular debris via centrifugation for 45 min at 35,000 \times g. The soluble pink lysate was purified with fast protein liquid chromatography as previously described for WT cyt P460.¹

Reactions of WT cyt P460 to form {FeNO}⁷ species. {FeNO}⁷ species were generated by either treating Fe^{III} cyt P460 with HNO generated by Na₂N₂O₃ or treating Fe^{II} cyt P460 with NO generated by Proli-NONOate. Fe^{III} cyt P460 (15 μ M) in 2 mL of deoxygenated 200 mM 4-(2-hydroxyethyl)-1-piperazine-ethanesulphonic acid (HEPES; pH 8.0) buffer was prepared in a septum-sealed anaerobic cuvette in the glovebox. The reactions were initiated by adding the HNO donor Na₂N₂O₃ via gas-tight syringe (Hamilton) through the cuvette septum to a final concentration of 100 μ M. The 6c-to-5c {FeNO}⁷ conversion was monitored using the full spectrum (200-800 nm) Cary 60 UV-vis spectrometer with scans at 0.5 min intervals from 0 to

10 min, 1 min intervals from 10 to 20 min, and 2 min intervals from 20 to 40 min and the decay trace was monitored at 452 nm. Alternatively, Fe^{III} cyt P460 (10 μM) in 2 mL of deoxygenated 200 mM HEPES buffer (pH 8.0) was reduced by treatment with 2 equiv of sodium dithionite (Na₂S₂O₄) in a septum-sealed anaerobic cuvette in the glovebox. The formation of the 6c {FeNO}⁷ species was initiated by adding 50 μM Proli-NONOate to generate 100 μM NO and monitored with UV-vis absorption scans as described above.

Reactions of the 6c and 5c {FeNO}⁷ species with NH₂OH or oxidant. All {FeNO}⁷ samples were prepared in the glovebox as described above. Solid NH₂OH•HCl was equilibrated under a N₂ atmosphere in the glovebox overnight. Then, 1 M NH₂OH•HCl solutions were prepared by dissolving the equilibrated solid into 1 mL of deoxygenated Milli-Q water. Solid [Ru(NH₃)₆]Cl₃ was equilibrated overnight in the glovebox and then dissolved in 1 mL of deoxygenated Milli-Q water to generate a 200 mM stock solution. The 6c {FeNO}⁷ species was generated using HNO from Fe^{III} cyt P460 as described above. After the maximal formation (approximately 2 min) of the 6c {FeNO}⁷ species, the reaction was monitored at 452 nm, NH₂OH•HCl or oxidant to concentrations listed in the figure captions were added via gas-tight syringe. The 5c {FeNO}⁷ species was generated from the reaction of Fe^{III} cyt P460 (10 μM) with 50 μM HNO generated by Na₂N₂O₃ in 2 mL of deoxygenated 200 mM HEPES buffer (pH 8.0) in a septum-sealed anaerobic cuvette in the glovebox. The species was incubated in the glovebox for approximately 30 min to effect complete conversion to the 5c form. The reaction between the 5c {FeNO}⁷ species and NH₂OH or oxidant was initiated similarly as described for the 6c {FeNO}⁷ species and monitored at 455 nm. The alternative oxidants dichlorophenolindophenol (DCPIP), phenazine methosulfate (PMS), potassium hexachloroiridate, and potassium ferricyanide were also tested; stocks solutions were prepared as described above.

Kinetic measurements of 6c-to-5c {FeNO}⁷ conversion. Kinetic studies of the 6c-to-5c {FeNO}⁷ conversion for the WT cyt P460 were monitored by UV-vis absorption spectroscopy. Fe^{II} or Fe^{III} cyt P460 solutions were in a septum-sealed cuvette and reactions were initiated by adding Proli-NONOate or Na₂N₂O₃, respectively, via gas-tight syringe. NO and HNO concentrations were varied between 100 and 600 μM by adding appropriate volumes of Proli-NONOate or Na₂N₂O₃ stock solutions. The reaction was monitored at 452 nm at 25 °C. A single-exponential equation was fit to the 452-nm kinetic traces. These fits provided observed rate constants (k_{obs}) at each NO and HNO concentration and were then plotted against these concentrations to evaluate order in either NO or HNO.

The kinetics of Lys70Tyr cyt P460 6c-to-5c {FeNO}⁷ conversion with varying HNO or NO concentrations were monitored by UV-vis absorption spectroscopy or stopped-flow UV-vis absorption spectroscopy, respectively. Reactions of Fe^{III} Lys70Tyr cyt P460 with varying HNO concentrations were performed as described for the WT cyt P460. Faster reactions of the Lys70Tyr mutant with NO were monitored using stopped-flow UV-vis absorption spectrophotometry. For stopped-flow experiments Proli-NONOate in 10mM NaOH was used as the NO generator and was shot against Fe^{II} Lys70Tyr in 200mM HEPES buffer pH 8.0 with final concentrations after mixing of 10 μM Lys70Tyr cyt P460, 50 μM Na₂S₂O₄, and varying NO in the range of 100–600 μM. All reactions were monitored at 415 nm at 25 °C. A single- or double-exponential equation was fit to the 415-nm kinetic traces. These fits provided observed rate constants ($k_{obs}=k[NO]$) at each NO concentration. The plots of k_{obs} versus NO concentration were fit with linear regression to obtain the rate constant k .

Temperature-dependent kinetic studies were performed for all species as described above while varying the temperature between 15 °C and 35 °C at 5 °C increments. Data was analyzed by non-linear regression also described above. Rate constants were plotted against the inverse of temperature (T) in K. Linear fits to these plots were used to extract values for activation enthalpy (ΔH^\ddagger) and activation entropy (ΔS^\ddagger) according to the Eyring³ equation (eq 1):

$$\ln \frac{k}{T} = \frac{-\Delta H^\ddagger}{R} \left(\frac{1}{T} \right) + \ln \left(\frac{k_B}{h} \right) + \frac{\Delta S^\ddagger}{R} \quad (1)$$

where k_B is the Boltzmann constant, h is Planck's constant, and R is the gas constant.

EPR measurements. Continuous-wave X-band (9.40 GHz) EPR spectra were recorded at the NIH Biomedical Center for Advanced ESR Technology (ACERT) using a Bruker Elexsys-II spectrometer equipped with a liquid He cryostat (Oxford Instruments). All samples were prepared in an anaerobic glovebox with deoxygenated solutions. The protein concentrations used were 0.15 mM in 200 mM HEPES buffer (pH 8.0) with 25% (v/v) glycerol. EPR data were simulated, and spin concentrations were determined with SpinCount.^{4, 5}

Fe K-edge X-ray absorption spectroscopy. Samples for Fe K-edge X-ray absorption spectroscopy (XAS) were prepared in an anaerobic glovebox with 1 mM protein and 25% (v/v) glycerol, loaded into a Delrin sample cell, and sealed with 37 μ m Kapton tape. The 5c WT cyt P460 {FeNO}⁷ sample was prepared by allowing 1 mM Fe^{III} P460 to react with 8 mM Na₂N₂O₃ for 30 min. The sample was then frozen in liquid N₂ outside of the box. The Lys70Tyr cyt P460 5c {FeNO}⁷ sample was prepared in the glovebox by treating 1 mM Lys70Tyr cyt P460 with 2 equiv of sodium dithionite and 10 mM Proli-NONOate. The sample was then frozen outside the glovebox in liquid N₂. The formation of the WT cyt P460 6c {FeNO}⁷ species was first monitored with UV-vis absorption spectroscopy to obtain a time course for maximum accumulation, which occurred within 3 min. In the glovebox, the Lys70Tyr cyt P460 6c {FeNO}⁷ species was prepared by treating 1 mM Fe^{III} Lys70Tyr cyt P460 with 4 mM Na₂N₂O₃ and freezing the mixture outside the glovebox in liquid N₂ within 3 min.

Fe K-edge XAS data including extended X-ray absorption fine structure (EXAFS) data were obtained at the Stanford Synchrotron Lightsource Radiation (SSRL) at the 16-pole, 2 T wiggler beamline 9-3 under ring conditions of 3 GeV and 500 mA. A Si(220) double-crystal monochromator was used for energy selection, and a Rh-coated mirror (set to an energy cutoff of 13 keV) was used for harmonic rejection. Internal energy calibration was performed by assigning the first inflection point of an Fe foil spectrum to 7111.2 eV. Data were collected in fluorescence mode (windowed onto Fe K α_1) using a Canberra 100-element Ge moonlight solid-state detector perpendicular to the incident beam. Elastic scatter into the detector was attenuated using a Soller slit with an upstream Mn filter. Data were collected from 6800 to 8000 eV ($k = 14 \text{ \AA}^{-1}$), and 16 scans were obtained for each sample. Multiple spots were collected per sample, although there was no evidence of photodamage. The scans were averaged and processed using the SIXPACK software package. A smooth pre-edge background was removed from each averaged spectrum by fitting a first-order polynomial to the pre-edge region and subtracting this polynomial from the

entire spectrum. The post-edge region was fit to a polynomial spline, flattened below 7130 eV, and then subtracted from the entire spectrum. Data were then normalized to a value of 1.0 at 7130 eV. EXAFS data were fit using the OPT module of the EXAFSPAK⁶ software package with input scattering paths generated using FEFF7.^{7,8}

Resonance Raman measurements. Resonance Raman (rR) spectra were obtained using a home-built spectrometer. Samples were prepared in J. Young NMR tubes in the glovebox. Samples were excited using either a SpectraPhysics Stabilite 1800 Ar/Kr mixed-gas laser or a 405 nm diffraction-limited Lepton IV diode laser (Microlaser Systems). Incident laser excitation was passed through Semrock MaxLine laser clean-up filters and focused to a ca. 2mm point using a spherical lens (ThorLabs). Samples were held in a 180° backscattering geometry and continuously spun at room temperature using an NMR tube spinner for power dissipation. Incident laser power at the sample was measured using a ThorLabs digital power meter. Scattered light was collected in a 180° backscattering geometry using a 50 mM Canon F/1.2 FD macro lens and focused through a 10 μm slit into an Princeton Instruments IsoPlane SCT320 spectrograph using an F-matched achromatic doublet lens. Semrock Razoredge long-pass filters were used to remove Rayleigh scattering. Scattered, filtered light was energy dispersed using either 1200 or 2400 g/mm gratings onto a Pixis 100B eXcelon digital CCD held thermoelectrically at -60 °C. Data were recorded and processed using the Lightfield software package (Princeton Instruments). Acetaminophen was used as a Raman shift calibrant.

Supplementary Figures

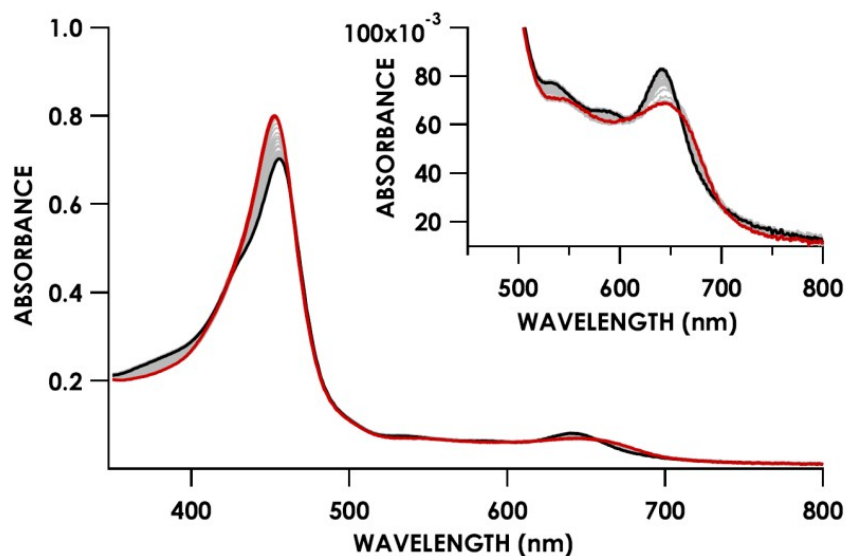


Figure S1. UV-vis absorption full-spectral scans of the reaction of 15 μM 6c {FeNO}⁷ and 10mM NH₂OH in 200mM HEPES pH 8.0. The solid red trace corresponds to the 6c {FeNO}⁷ after addition of 10mM NH₂OH. Grey spectra are collected in 30s increments for 30 min and the black spectra is the final species corresponding to the 5c {FeNO}⁷. Inset highlights the q band region after the addition of NH₂OH and corresponds to the transition from the 6c to 5c {FeNO}⁷.

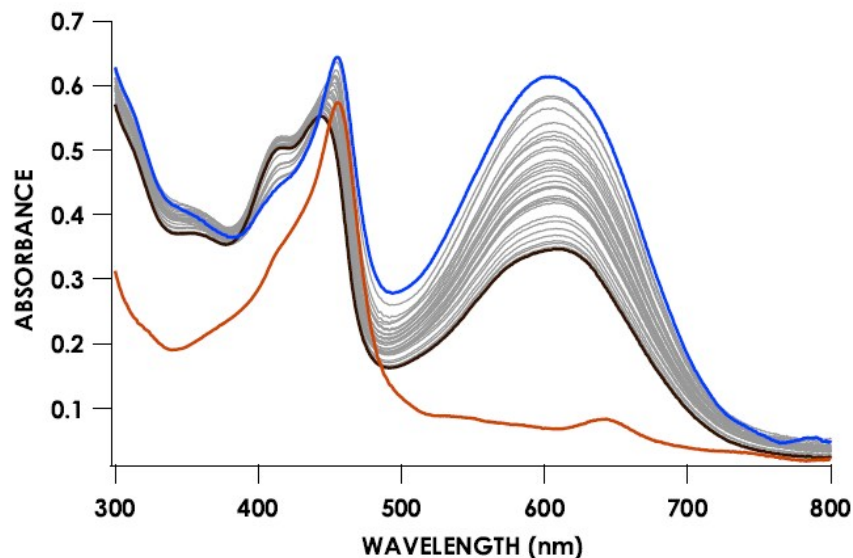


Figure S2. UV-vis absorption full-spectral scans of the reaction of 5c {FeNO}⁷ species formed by treatment of 15 μM Fe^{III} and 100 μM of the HNO donor Na₂N₂O₃ and allowed to react for 30 mins in 200mM HEPES pH 8.0. The solid red trace corresponds to the 5c {FeNO}⁷ prior to the addition of the oxidant dichloroindolphenol (DCPIP). The solid blue trace is immediately after addition of 1mM DCPIP. Grey spectra are collected in 30s increments for 20 min and the black spectra is the final species with a split soret max at 413 nm and 442 nm.

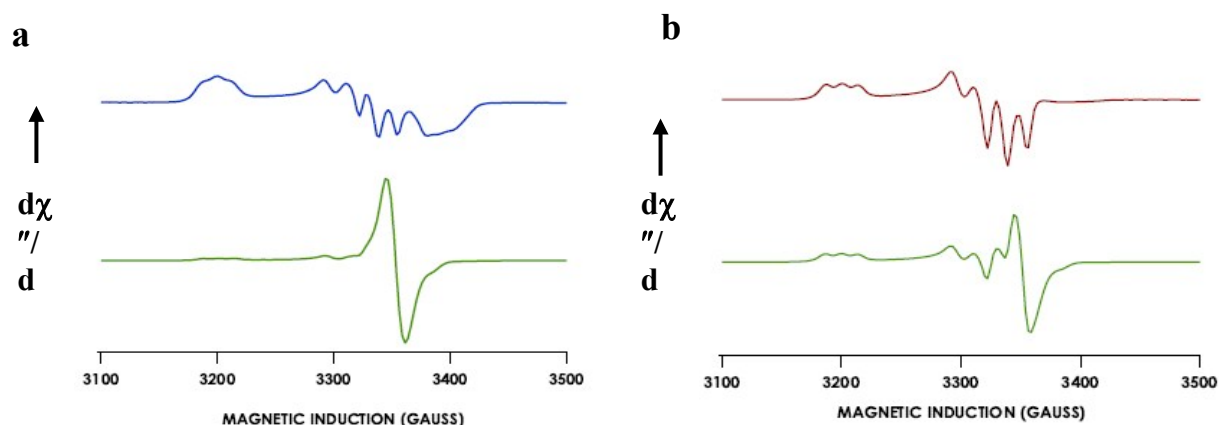


Figure S3. EPR spectra of 200 μM P460 Fe^{III} cyt P460 with the addition of 1mM of the HNO donor $\text{Na}_2\text{N}_2\text{O}_3$ at room temperature for a) 2 min (blue trace) or b) 30 min (red trace) and subsequently reacted with 800 μM of the oxidant phenazine methosulfate (green traces).

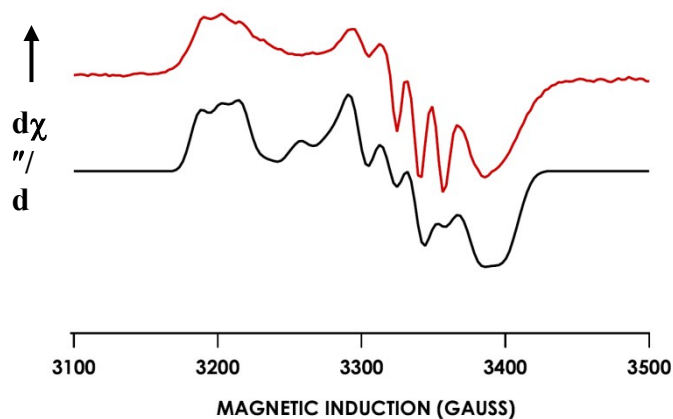


Figure S4. EPR spectrum shown in red of 200 μM P460 treated with 1 mM NH_2OH and 1 mM dichlorophenolindophenol (DCPIP) in 200 mM HEPES buffer (pH 8.0). The sample was frozen 2 min after the consumption of oxidant. The black spectrum is the corresponding simulation of the $\text{Fe}^{\text{III}}\text{-NH}_2\text{OH}$ oxidized species and is consistent with the 6c $\{\text{FeNO}\}^7$ generated from either addition of HNO or NO to Fe^{III} and Fe^{II} , respectively.

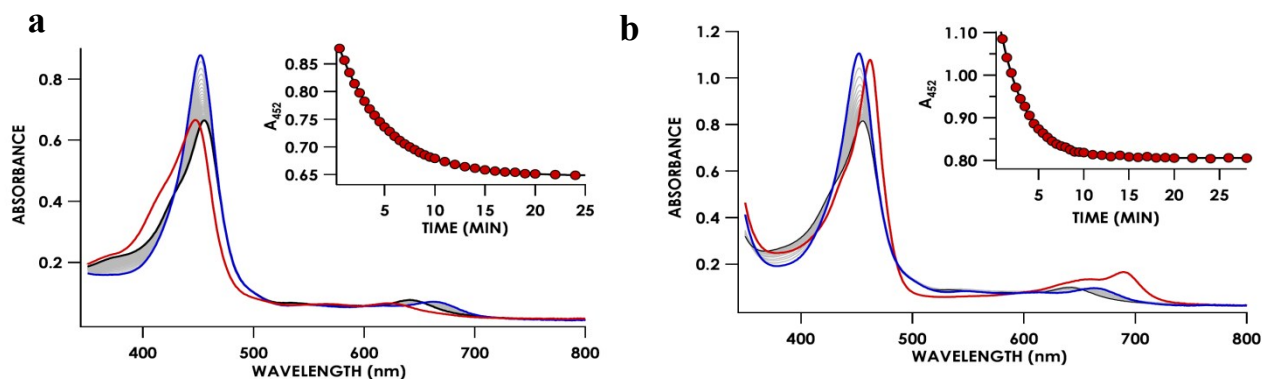


Figure S5. UV-vis absorption full-spectral scans of the reaction of cyt P460 15 μ M (a) Fe^{III} and 100 μ M of the HNO donor Na₂N₂O₃ or (b) Fe^{II} with 100 μ M NO (50 μ M Proli-NONOate). The red trace is the initial species of (a) Fe^{III} or (b) Fe^{II}. The blue trace is after the addition of (a) HNO or (b) NO and black is the final trace of the 5c {FeNO}⁷. The insert is the corresponding single wavelength time course following the absorbance at 452 nm.

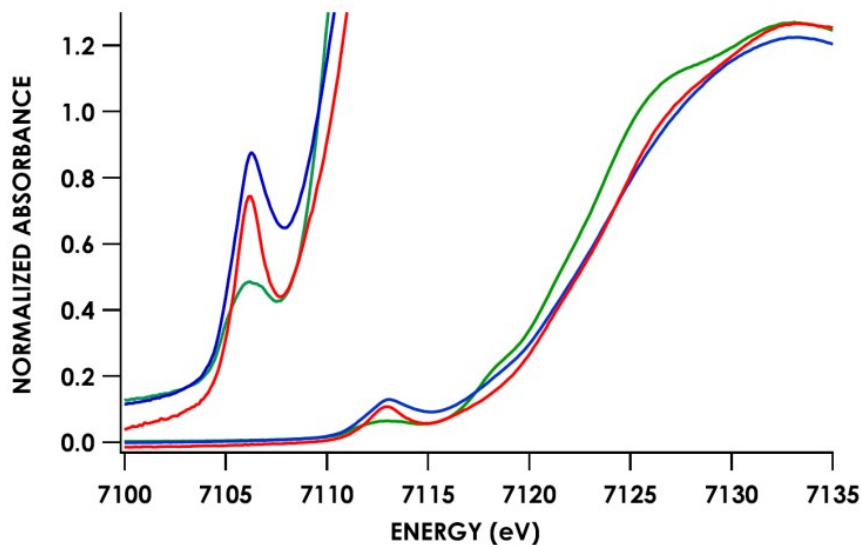


Figure S6. Fe-K edge X-ray absorption spectra (XAS) obtained at 10 K of 1mM Fe^{II} Lys70Tyr treated with 10mM NO immediately frozen to form the Lys70Tyr 5c {FeNO}⁷ species (red trace). The Lys70Tyr 5c {FeNO}⁷ species is compared to the 6c (green trace) and 5c (blue trace) WT cyt P460 {FeNO}⁷ species. All samples were glassed in 200mM HEPES buffer pH 8.0 with 25% v/v glycerol. The 1s \rightarrow 3d pre-edge feature is at 7113.3 eV.

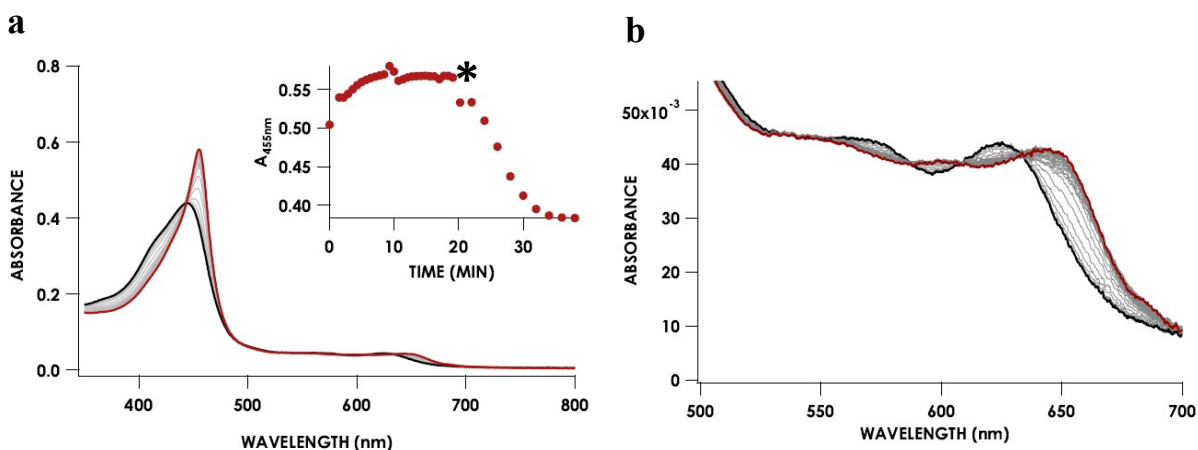


Figure S7. UV-vis absorption full-spectral scans (a) of the reaction of cyt P460 15 μ M Fe^{III} and 100 μ M of the HNO donor Na₂N₂O₃ after the addition of 100 μ M Ru(NH₃)₆Cl₃ (red trace) to form the {FeNO}⁶ intermediate. The gray spectra were collected in 30s increments for 40 min and the black spectra corresponds to the Fe^{III} complex. The insert is the corresponding single wavelength time course following the absorbance at 455 nm and the * indicates the addition of 1mM HA after maximal formation of the {FeNO}⁶ species. (b) Highlights the q bands following the transition from the {FeNO}⁶ to the Fe^{III} complex.

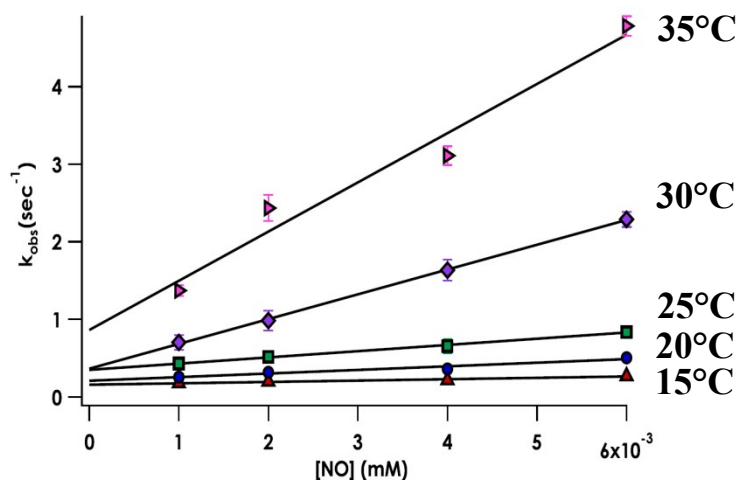


Figure S8. Plots of k_{obs} versus NO concentration as a function of temperature for the reaction of Fe^{II} Lys70Tyr cyt P460 and NO.

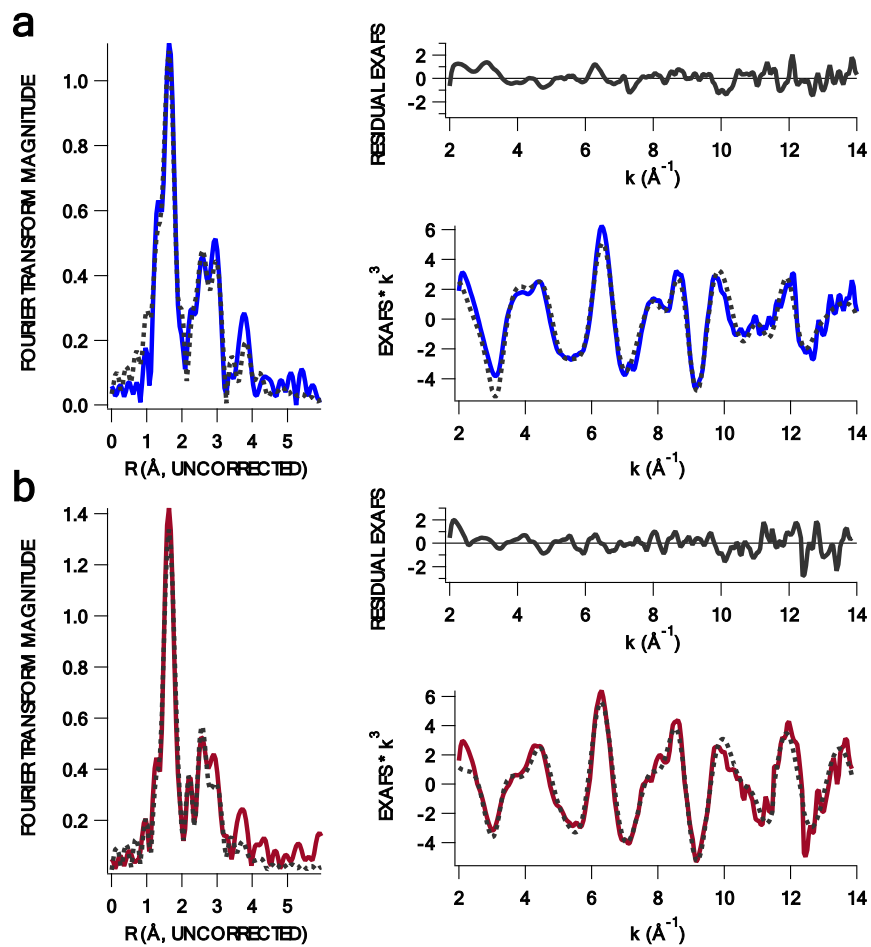


Figure S9. Fe K-edge EXAFS data obtained at 10 K for the 6c (a) and 5c (b) cyt P460 {FeNO}₇ intermediates in glassed 200 mM HEPES buffer (pH 8.0) containing 25% v/v glycerol. Experimental data are plotted as solid lines; fits are dotted lines.

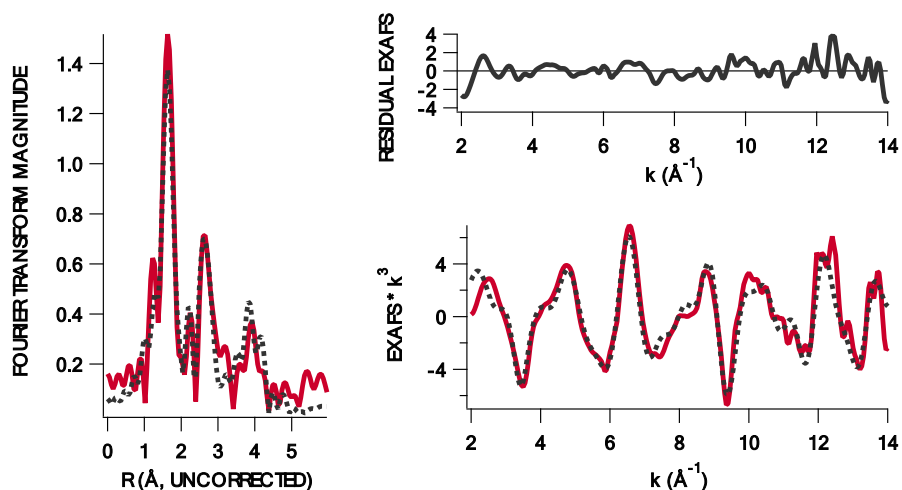


Figure S10. Fe K-edge EXAFS data obtained at 10 K for Lys70Tyr cyt P460 5c {FeNO}⁷ in glassed 200 mM HEPES buffer (pH 8.0) containing 25% v/v glycerol. Experimental data are plotted as solid lines; fits are dotted lines.

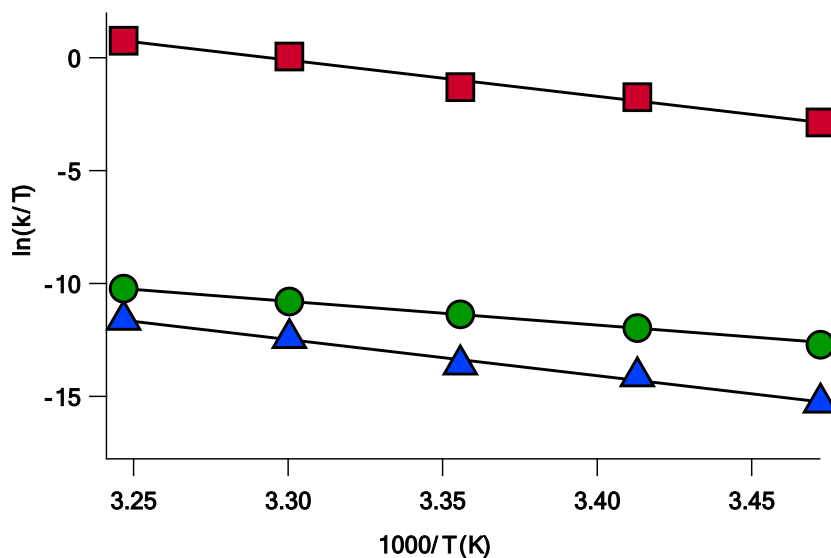


Figure S11. Eyring plots of $\ln(k_{His-off}/T)$ for WT (green circles) and Lys70Tyr (blue triangles) cyt P460 {FeNO}⁷ species and $\ln[k_{His-off}(NO)/T]$ for Lys70Tyr cyt P460 (red squares) vs $1000/T$. Rate constants and activation parameters appear in Table 3.

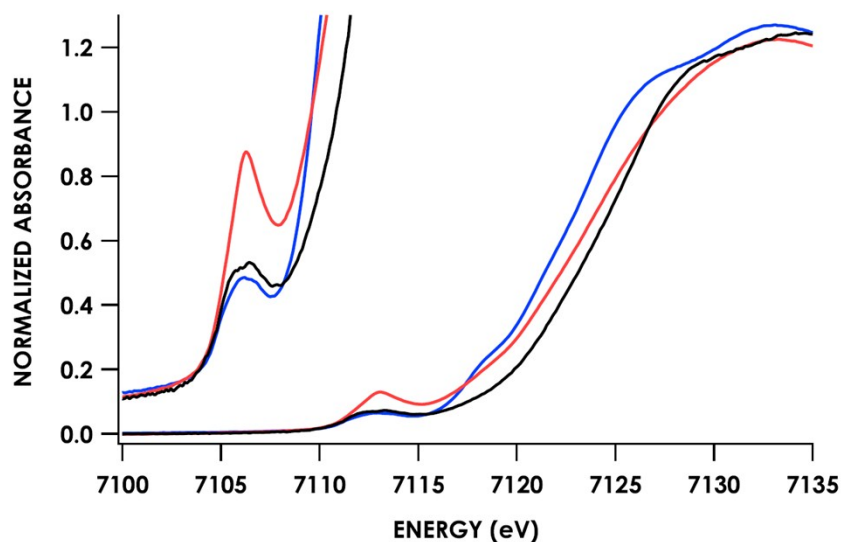


Figure S12. Fe-K edge X-ray absorption spectra (XAS) obtained at 10 K of 1mM Fe^{III} WT cyt P460 treated with 10mM NO immediately frozen to form the {FeNO}⁶ species (black trace). The {FeNO}⁶ species is compared to the 6c (blue trace) and 5c (red trace) WT cyt P460 {FeNO}⁷ species. All samples were glassed in 200mM HEPES buffer pH 8.0 with 25% v/v glycerol. The 1s → 3d pre-edge feature is at 7113.3 eV.

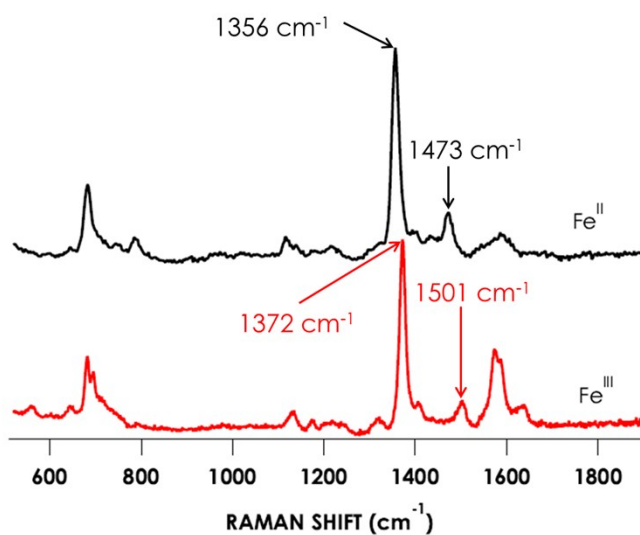


Figure S13. The rR spectra obtained via near-resonance excitation with Soret absorption band: $\lambda_{\text{ex}} = 405.0$ nm (20 mW) for Ly70Tyr Fe^{II} (black) and Fe^{III} (red) the $\nu(4)$ and $\nu(3)$ are labeled above.

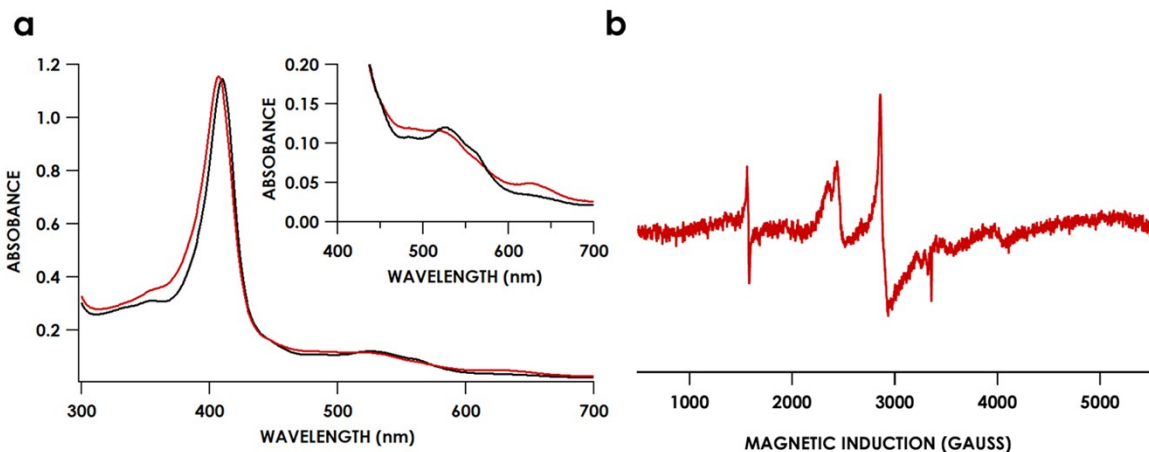


Figure S14. UV-vis absorption spectrum (a) of 10 μ M K70Y with the addition of 20mM NH_2OH in 200mM HEPES buffer pH 8.0 and EPR spectrum (b) of 200 μ M Lys70Tyr treated with 100 mM NH_2OH prepared in 200mM HEPES buffer pH 8.0 with 25% glycerol.

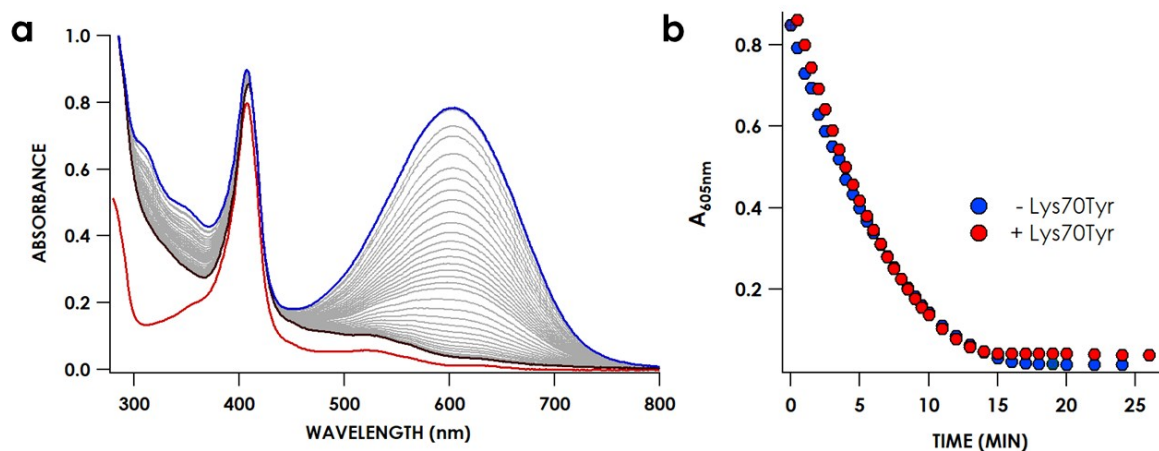


Figure S15. UV-vis absorption spectrum (a) of 10 μ M K70Y with 15mM NH_2OH and the addition of 100 μ M DCPIP in 200mM HEPES buffer pH 8.0 and (b) the corresponding single wavelength time course following the consumption of DCPIP with conditions of 100 μ M DCPIP and 15mM NH_2OH either in the presence or absence of 10 μ M K70Y.

Supplementary Tables

Table S1. EXAFS simulations for cyt P460 6c {FeNO}⁷ EXAFS data were fit with EXAFSPAK using paths calculated by FEFF7. Distance and Debye-Waller factors were allowed to float while, coordination numbers were held constant. Goodness of fit is determined by F, defined as $[(\text{EXAFS}_{\text{abs}} - \text{EXAFS}_{\text{calc}})_i^2/n]^{1/2}$. Fe-N_p denotes the pyrrole nitrogens of the porphyrin, Fe-C_α denotes the α carbons of the porphyrin, Fe-C_{meso} denotes the meso carbons of the porphyrin and Fe-C_β denotes the β carbons of the porphyrin.

Fit	Path	Coordination #	R(Å)	±	σ ²	±	F
1	Fe-N _p	5	2.038	0.0047	0.0062	0.0004	60.40%
2	Fe-N _p	5	2.029	0.0056	0.0049	0.0004	
	Fe-N(NO)	1	1.849	0.0185	0.0054	0.0021	58.99%
3	Fe-N _p	5	2.043	0.0028	0.0060	0.0003	
	Fe-N(NO)	1	1.647	0.0307	0.0252	0.0070	
	Fe-C _α	8	3.041	0.0051	0.0053	0.0005	43.02%
4	Fe-N _p	5	2.044	0.0023	0.0061	0.0002	
	Fe-NO	1	1.650	0.0270	0.0266	0.0059	
	Fe-C _α	8	3.042	0.0045	0.0058	0.0004	
	Fe-C _{meso}	4	3.376	0.0045	0.0058	0.0004	33.05%
5	Fe-N _p	5	2.037	0.0027	0.0048	0.0003	
	Fe-C _α	8	3.020	0.0045	0.0063	0.0005	
	Fe-C _{meso}	4	3.364	0.0044	0.0015	0.0004	
	Fe-N(NO)	1	1.862	0.0108	0.0058	0.0013	
	Fe-C _β	8	4.446	0.0122	0.0066	0.0013	32.45%
6	Fe-N _p	5	2.037	0.0024	0.0050	0.0002	
	Fe-C _α	8	3.026	0.0041	0.0063	0.0004	
	Fe-C _{meso}	4	3.364	0.0041	0.0016	0.0004	
	Fe-N(NO)	1	1.858	0.0117	0.0074	0.0015	
	Fe-C _β	16	4.334	0.0084	0.0006	0.0009	29.58%

Table S2. EXAFS simulations for cyt P460 5c {FeNO}⁷ EXAFS data were fit with EXAFSPAK using paths calculated by FEFF7. Distance and Debye-Waller factors were allowed to float while, coordination numbers were held constant. Goodness of fit is determined by F, defined as $[(\text{EXAFS}_{\text{abs}} - \text{EXAFS}_{\text{calc}})_i^2/n]^{1/2}$. Fe-N_p denotes the pyrrole nitrogens of the porphyrin, Fe-C_α denotes the α carbons of the porphyrin, Fe-C_{meso} denotes the meso carbons of the porphyrin and Fe-C_β denotes the β carbons of the porphyrin.

Fit	Path	Coordination #	R(Å)	±	σ ²	±	F
1	Fe-N _p	4	2.020	0.0034	0.0028	0.0002	55.04%
2	Fe-N _p	4	2.023	0.0022	0.0028	0.0002	
	Fe-C _α	8	3.036	0.0052	0.0050	0.0005	41.28%
3	Fe-N _p	5	2.023	0.0025	0.0040	0.0002	
	Fe-C _α	8	3.033	0.0056	0.0050	0.0006	45.91%
4	Fe-N _p	4	2.022	0.0022	0.0027	0.0005	
	Fe-C _α	8	3.036	0.0050	0.0051	0.0005	
	Fe-N(NO)	1	1.723	0.0233	0.0161	0.0042	38.05%
5	Fe-N _p	4	2.024	0.0021	0.0028	0.0002	
	Fe-C _α	8	3.039	0.0049	0.0052	0.0004	
	Fe-N(NO)	1	1.715	0.0226	0.0171	0.0039	
	Fe-C _{meso}	4	3.389	0.0151	0.0053	0.0011	33.48%
6	Fe-N _p	4	2.025	0.0020	0.0028	0.0002	
	Fe-C _α	8	3.041	0.0047	0.0053	0.0004	
	Fe-N(NO)	1	1.703	0.0181	0.0181	0.0041	
	Fe-C _{meso}	4	3.395	0.0048	0.0050	0.0011	
	Fe-N(His)	1	2.533	0.0137	0.0042	0.0015	32.42%
8	Fe-N _p	4	2.021	0.0020	0.0027	0.0001	
	Fe-C _α	8	3.032	0.0048	0.0054	0.0004	
	Fe-N(NO)	1	1.742	0.0255	0.0189	0.0045	
	Fe-C _{meso}	4	3.382	0.0087	0.0043	0.0009	
	Fe-C _β	16	4.381	0.0200	0.0059	0.0027	
	Fe-N(His)	1	2.524	0.0125	0.0039	0.0013	31.23%
9	Fe-N _p	4	2.021	0.0020	0.0027	0.0002	
	Fe-C _α	8	3.028	0.0047	0.0053	0.0004	
	Fe-N(NO)	0.75	1.735	0.0227	0.0129	0.0036	
	Fe-C _{meso}	4	3.384	0.0088	0.0044	0.0009	
	Fe-C _β	16	4.385	0.1995	0.0060	0.0028	
	Fe-N(His)	1	2.525	0.0124	0.0038	0.0013	30.25%

Table S3. EXAFS simulations for Lys70Tyr cyt P460 5c {FeNO}⁷ EXAFS data were fit with EXAFSPAK using paths calculated by FEFF7. Distance and Debye-Waller factors were allowed to float while, coordination numbers were held constant. Goodness of fit is determined by F, defined as $[(\text{EXAFS}_{\text{abs}} - \text{EXAFS}_{\text{calc}})_i^2/n]^{1/2}$. Fe-N_p denotes the pyrrole nitrogens of the porphyrin, Fe-C_α denotes the α carbons of the porphyrin, Fe-MS denotes carbon nitrogen multiscatters and Fe-C_β denotes the β carbons of the porphyrin.

Fit	Path	Coordination #	R(Å)	±	σ ²	±	F
1	Fe-N _p	4	1.998	0.0038	0.0033	0.0003	60.54%
2	Fe-N _p	4	2.009	0.0029	0.0035	0.0003	
3	Fe-C _α	8	2.977	0.0061	0.0039	0.0005	55.84%
	Fe-N _p	5	2.009	0.0032	0.0050	0.0035	
4	Fe-C _α	8	2.968	0.0066	0.0038	0.0006	61.34%
	Fe-N _p	4	1.990	0.0038	0.0030	0.0003	
5	Fe-C _α	8	3.002	0.0054	0.0039	0.0005	52.44%
	Fe-N(NO)	1	1.776	0.0156	0.0056	0.0018	
	Fe-N _p	4	1.992	0.0037	0.0030	0.0003	
6	Fe-C _α	8	3.000	0.0055	0.0041	0.0006	51.01%
	Fe-N(NO)	1	1.788	0.0194	0.0073	0.0025	
	Fe-N(His)	1	2.502	0.0156	0.0023	0.0016	
	Fe-N _p	4	1.995	0.0030	0.0030	0.0003	
7	Fe-C _α	8	3.000	0.0044	0.0037	0.0004	40.66%
	Fe-N(NO)	1	1.807	0.0185	0.0086	0.0026	
	Fe-N(His)	1	2.490	0.0115	0.0019	0.0012	
	Fe-MS	16	3.233	0.0132	0.0025	0.0017	
	Fe-N _p	4	1.991	0.0025	0.0028	0.0002	
8	Fe-C _α	8	2.997	0.0038	0.0038	0.0003	35.66%
	Fe-N(NO)	1	1.805	0.0141	0.0069	0.0018	
	Fe-N(His)	8	2.483	0.0117	0.0026	0.0012	
	Fe-MS	16	3.224	0.0114	0.0022	0.0014	
	Fe-C _β	8	4.341	0.0055	0.0020	0.0005	

References

1. J. D. Caranto, A. C. Vilbert and K. M. Lancaster, *Proc. Natl. Acad. Sci. U.S.A.*, 2016, **113**, 14704-14709.
2. L. Thöny-Meyer, F. Fischer, P. Künzler, D. Ritz and H. Hennecke, *J. Bacteriol.*, 1995, **177**, 4321-4326.
3. H. Eyring, *J. Chem. Phys.*, 1935, **3**, 107-115.
4. A. P. Golombek and M. P. Hendrich, *J. Magn. Reson.*, 2003, **165**, 33-48.
5. D. T. Petasis and M. P. Hendrich, *Methods Enzymol.*, 2015, **563**, 171-208.
6. G. N. George, *Journal*, 2001.
7. J. Mustre de Leon, J. J. Rehr, S. I. Zabinsky and R. C. Albers, *Phys. Rev. B.*, 1991, **44**, 4146-4156.
8. J. J. Rehr, J. Mustre de Leon, S. I. Zabinsky and R. C. Albers, *J. Am. Chem. Soc.*, 1991, **113**, 5135-5140.